Synthetic-lethal Interactions Identify Two Novel Genes, *SLA1* and *SLA2*, That Control Membrane Cytoskeleton Assembly in *Saccharomyces cerevisiae*

Douglas A. Holtzman, Shirley Yang, and David G. Drubin

Department of Molecular and Cell Biology, University of California, Berkeley, California 94720

Abstract. Abplp is a yeast cortical actin-binding protein that contains an SH3 domain similar to those found in signal transduction proteins that function at the membrane/cytoskeleton interface. Although no detectable phenotypes are associated with a disruption allele of *ABP1*, mutations that create a requirement for this protein have now been isolated in the previously identified gene *SAC6* and in two new genes, *SLA1* and *SLA2*. The *SAC6* gene encodes yeast fimbrin, an actin filament-bundling protein. Null mutations in *SLA1* and *SLA2* cause temperature-sensitive growth defects. Slalp contains three SH3 domains and is essential for the proper formation of the cortical actin cytoskeleton. The COOH terminus of Sla2p contains a 200 amino acid region with homology to the COOH terminus of talin, a membrane cytoskeletal protein which is a component of fibroblast focal adhesions. Sla2p is required for cellular morphogenesis and polarization of the cortical cytoskeleton. In addition, synthetic-lethal interactions were observed for double-mutants containing null alleles of *SLA2* and *SAC6*. In total, the mutant phenotypes, sequences, and genetic interactions indicate that we have identified novel proteins that cooperate to control the dynamic cytoskeletal rearrangements that are required for the development of cell polarity in budding yeast.

THE cortical actin cytoskeleton underlies the plasma membrane and is responsible for cell motility and adhesion, surface phenomena such as membrane ruffling and receptor capping, and transduction of extracellular signals to the interior of the cell (reviewed by Luna and Hitt, 1992; Schwartz, 1992). Genetic defects in components of the cortical cytoskeleton can lead to disease states, including muscular dystrophy and certain hereditary anemias (reviewed by Luna and Hitt, 1992). A complete understanding of how the cortical cytoskeleton functions in these processes is hampered by its complexity; a large number of cortical cytoskeletal proteins are known, and it is probable that there are others as yet unidentified. However, even if a thorough characterization of the in vitro activities of each protein could be achieved, it is unlikely that this would provide a complete understanding of how the actin cytoskeleton influences cell behavior. One reason for this is that there are likely to be a host of regulatory as well as competetive and cooperative interactions that may be difficult to model in vitro. Moreover, molecular-genetic studies have shown that the in vivo contributions of individual cytoskeletal proteins can be more subtle than previously supposed (De Lozanne and Spudich, 1987; Witke et al., 1992; Adams et al., 1993), adding an additional obstacle to understanding the cortical cytoskeleton.

Saccharomyces cerevisiae has a single actin gene, *ACT1*, that is ~90% identical to most vertebrate actins (Ng and Abelson, 1980; Gallwitz and Sures, 1980) and is essential for the polarized growth of the cell (Novick and Botstein, 1985; Read et al., 1992). Wild-type cells initiate daughter cell formation by choosing a bud site and confining surface growth to this region. Two different actin structures have been identified in budding yeast through fluorescence microscopy techniques (Adams and Pringle, 1984), and both are likely to contribute to morphogenesis. Actin cables are arrayed parallel to the mother-bud axis and might be involved in the spatially directed secretion (Field and Schekman, 1980) that is essential for the polarized growth of the yeast cell. In addition, cortical actin structures are found associated with the growing surfaces of the cell, and the localization of these structures changes in a cell cycle-dependent manner (Kilmartin and Adams, 1984). The phenotypes of mutants defective in the polarized assembly of the yeast cortical cytoskeleton demonstrate a role for these structures in cellular morphogenesis (Novick and Botstein, 1985; Adams et al., 1989, 1990; Amatruda et al., 1990; Read et al., 1992).

One component of the yeast cortical cytoskeleton is the 65-kD product of the *ABP1* gene (Drubin et al., 1988). The NH_2 terminus of Abplp shares 41% similarity with yeast cofilin, a low molecular weight actin filament-severing protein (Moon et al., 1993), while its COOH termi-

nus contains a 50 amino acid region termed the src-homology domain 3 (SH3)[1] (Drubin et al., 1990). This motif is found in a large and diverse group of proteins that appear to interact with the cortical cytoskeleton (Koch et al., 1991). *BEM1*, a gene required for morphogenesis in *S. cerevisiae*, contains two SH3 domains (Chenevert et al., 1992), providing an indication that this sequence element might be involved in cell polarity development. Interestingly, the SH3 domains of both the c-abl and c-src proto-oncogenes have been shown recently to bind specifically to 3BP-1, a protein which has homology to rho-GTPase activators of the bcr/N-chimaerin family (Cicchetti et al., 1992; Yu et al., 1992). Proteins of this class might mediate interactions between GTP-binding proteins implicated in polarity development (reviewed by Drubin, 1991) and the cytoskeleton via the SH3 domains of Abplp and/or Bemlp.

Overexpression of *ABP1* grossly perturbs the cytoskeleton (Drubin et al., 1988). Cells with elevated Abplp levels are temperature sensitive (Ts^-) for their growth and become large and spherical, losing the polarity found in wild-type cells. These studies, along with immunolocalization of Abplp to regions of active cell surface growth, implicated this protein in the polarized growth of *S. cerevisiae*. However, when the *ABP1* gene was disrupted, the mutant cells showed no defects in morphogenesis nor any discernable loss of cytoskeletal polarity (Drubin et al., 1990). These results suggested that there might be another gene product(s) in yeast that compensates for the loss of Abplp.

In an attempt to isolate more components of the membrane cytoskeleton, and to elucidate the molecular mechanisms of cellular morphogenesis, we have undertaken a genetic screen to identify mutations that create a requirement for *ABP1*. This strategy, termed a synthetic lethal screen, has been useful for the identification of genes that are involved in a common process (Bender and Pringle, 1991). Mutations that create a requirement for *ABP1* were isolated in three genes. One of these genes, *SAC6*, encodes the yeast homolog of fimbrin (Adams et al., 1989). The two other genes, *SLA1* and *SLA2* (Synthetically Lethal with ABP1) encode novel proteins. The phenotypes of null mutations in *SLA1* and *SLA2* show that these genes are essential for the assembly and function of the cortical cytoskeleton. Furthermore, the *SLA1* and *SLA2* sequences suggest protein interactions that might allow each gene product to regulate cortical actin cytoskeleton assembly.

Materials and Methods

Yeast Methods and DNA Manipulations

Yeast media and genetic manipulations were performed as described (Sherman et al., 1986). Yeast strains used in this study are listed in Table I. Plasmid DNA manipulations were carried out using standard methods (Ausubel et al., 1989).

Mutant Isolation

The *sla* mutants were isolated using a synthetic lethal strategy based on selection against the *LYS2* and *URA3* genes (Basson et al., 1987). DDY 262 (Table I) contains a nearly complete disruption of the *ABP1* gene (extending from an XhoI site 227-bp upstream of the start codon to a PvuII site 246-bp upstream of the stop codon, thus leaving only the last 82 amino acids at the COOH terminus intact, see Drubin et al., 1990), and a centromere-based plasmid (pDD13) which contains the *URA3*, *LYS2*, and *ABP1* genes. A stationary culture of DDY 262 was mutagenized with ethylmethanesulfonate until only 15% of the cells were viable. Approximately 25,000 colonies were plated onto 100 YPD plates and then replica plated onto plates containing α-aminoadipate to select against the *LYS2* gene as described (Sherman et al., 1986). After 3 d, colonies which failed to grow on the α-amino adipate plates were picked from the master plate and streaked to single colonies on YPD plates. These strains were then tested for their ability to grow on plates containing 5-Fluoro-orotic acid (5-FOA), to select against the *URA3* gene (Boeke et al., 1984). Colonies which failed to grow under both selections were backcrossed three times to the unmutagenized parent strain (DDY 262 or DDY 277) before the complementation analysis was performed.

Table I. Yeast Strains Used in This Study

Name	Genotype*
DDY 262	*MATa ade2-101 leu2-3,112 lys2-801am ura3-52 abp1-Δ2::LEU2*‡
DDY 277	*MATα his4-619 leu2-3,112 lys2-801am ura3-52 abp1-Δ2::LEU2*‡
DDY 538	*MATa leu2-3,112 lys2-801am ura3-52 sla1-3*
DDY 539	*MATa ade2-101 his4-619 leu2-3,112 lys2-801am ura3-52 sla2-2*
DDY 296	*MATa leu2-3,112 ura3-52 SLA1::URA3*
DDY 494	*MATa leu2-3,112 ura3-52*
DDY 495	*MATa leu2-3,112 ura3-52 sla1-Δ1::URA3*
DDY 496	*MATa leu2-3,112 ura3-52 sla2-Δ1::URA3*
DDY 288	*MATa/α his4-619/+ leu2-3,112/+ ura3-52/ura3-52*
DDY 485	*MATa/α his4-619/+ leu2-3,112/+ ura3-52/ura3-52 sla1-Δ1::URA3/sla1-Δ1::URA3*
DDY 540	*MATa/α his4-619/+ leu2-3,112/+ ura3-52/ura3-52 sla2-Δ1::URA3/sla2-Δ1::URA3*

* All strains are derived from the S288C background.
‡ Strains were transformed with a centromere plasmid pDD13 (*URA3*, *LYS2*, *ABP1*).

Complementation Analysis

Strains containing all possible double-mutant combinations were generated by mating plasmid-dependent *MATa ade2-101 ura3-52 leu2-3,112 lys2-80lam abp1::LEU2 sla* and *MATα his4-619 leu2-3,112 lys2-80lam ura3-52 abp1::LEU2 sla* strains, and selecting for diploids on minimal media (SD) plates supplemented with uracil and lysine to allow for the loss of pDD13. These strains were then replica plated to YPD plates and incubated at 37°C, and to YPD, α-aminoadipate and 5-FOA plates at 25°C. Plates were examined for growth at 36 h (37°C), 48 h (YPD 25°C), or 72 h (α-aminoadipate and 5-FOA, 25°C).

Cloning, Sequencing, and Disruption of SLA1 and SLA2

A YCp50 library (Rose et al., 1987) was introduced into the well-behaved Ts^- *sla1-3* and *sla2-2* strains, DDY 538 and DDY 539, by lithium acetate transformation (Ito et al., 1983; Schiestl and Gietz, 1989). The Ura^+ transformants were then replica plated onto SD plates lacking uracil and incubated at 37°C for 36 h. Colonies that grew well at 37°C were restreaked and tested for their ability to grow on both SD and 5-FOA plates at 37°C. Nine *sla1-3* and two *sla2-2* colonies displayed plasmid-dependent growth at 37°C. Plasmids from these strains were recovered by preparing DNA from the Ts^+ colonies, and transforming competent DH5α *E. coli* to ampicillin resistance. The plasmid DNAs were then retransformed into the appropriate strain to confirm their ability to complement the Ts^- phenotypes of the *sla1-3* and *sla2-2* strains, respectively. Eight of the nine *sla1*-complementing plasmids were shown to be identical based on restriction mapping, and the remaining plasmid contained a smaller insert that was contained entirely within the other plasmid. The two *sla2*-complementing plasmids shared restriction fragments, and this information was used to identify the *SLA2* open reading frame. DNA sequences were determined using the dideoxy chain

1. *Abbreviations used in this paper*: Cs^-, cold-sensitive; DAPI, (4',6-diamidino-2-phenyl-indole); 5-FOA, 5-Fluoro-orotic acid; SD, synthetic minimal media; SH3, src-homology domain 3; Ts-, temperature-sensitive.

termination method (Sanger et al., 1977) using Sequenase (United States Biochemical, Cleveland, OH) according to the suggested protocol of the manufacturer. *SLA1* was sequenced using an Exonuclease III deletion strategy and double-stranded plasmid DNA preparations; *SLA2* was sequenced by subcloning fragments into double stranded M13 phage and generating single-stranded DNA templates (Ausubel et al., 1989). Linkage of the cloned DNA to the *SLA1* locus was demonstrated by integrating the URA3 gene into the chromosome adjacent to the open reading frame and mating this strain (DDY 296) to two different Ts^- *sla1* mutations. All of the 44 tetrads dissected from the matings showed linkage (2:2, Ts^+, Ura^+: Ts^-, Ura^-). For *SLA2*, a gene disruption mutant (described below) was mated to an *sla2* mutant isolated in the genetic screen, and the diploid was then sporulated. A total of 11 complete tetrads and seven tetrads which had three viable spores were scored, and in all cases the spores were temperature sensitive, demonstrating linkage between the cloned DNA and the *sla2* mutation.

A complete disruption of the *SLA1* gene, including 409 nucleotides 5′ to the NH_2-terminal methionine and 213 nucleotides 3′ to the stop codon (from XbaI at position 49 through SalI at position 4402 in the *SLA1* gene sequence), was generated using the "γ-disruption" strategy with pRS306, a yeast integrating plasmid that contains the *URA3* gene (Sikorski and Hieter, 1989). While it is possible that this disruption might interfere with the expression of neighboring genes, the cortical defects of the *sla1* deletion strain (see Results) are the same as those observed in the Ts^- *sla1* mutants isolated in the genetic screen (data not shown), and no additional phenotypes were observed in the null mutant. The disruption of *SLA2* removes all but the first 30 amino acids of the coding sequence (from the SphI site at position 862 through the BclI at position 3675, which includes the stop codon of the *SLA2* gene sequence) by a simple one step gene replacement (Rothstein, 1983). Briefly, a plasmid containing the *SLA2* gene on a 4.5-kb EcoRI fragment was digested with SphI and treated with T4 DNA Polymerase before BclI linkers were ligated onto the ends. This plasmid was then digested with BclI, and a 1.1-kb BglII fragment containing the *URA3* gene was ligated to generate the disruption fragment. The resulting plasmid was then digested with EcoRI and transformed into DDY 288, a wild-type diploid strain. Both gene disruptions were confirmed by Southern blotting techniques (Ausubel et al., 1989).

Microscopy

Yeast cells grown to early log phase in YPD were prepared for immunofluorescence as previously described (Pringle et al., 1991). Affinity-purified rabbit anti-actin antibodies were used at a 1:50 dilution and visualized using fluorescein-labeled goat anti-rabbit secondary antibodies (Cappel/Organon Teknika, Malvern, PA) at a dilution of 1:1,000. Cells were photographed with a Zeiss Axioscope fluorescence microscope with an HB100 W/Z high pressure mercury lamp and a Zeiss 100× Plan-Neofluar oil immersion objective (Carl Zeiss Inc., Thornwood, NY) with either phase or Nomarski optics.

Results

Isolation of ABP1-requiring Mutants

The strategy that we used to isolate mutations that require *ABP1* relies on the ability to select against the *URA3* and *LYS2* genes with 5-FOA and α-aminoadipate, respectively (Boeke et al., 1984; Chattoo and Sherman, 1979), and on the fact that in the absence of positive selection, centromere-based plasmids are lost from a small percentage of the cells that form a colony (Basson et al., 1987). The starting haploid strain, DDY 262 (Table I), contains a complete disruption of *ABP1* (see Materials and Methods). Additionally, this strain was transformed with pDD13, a centromere-based plasmid that contains the *ABP1*, *URA3*, and *LYS2* genes. The population of cells that loses the plasmid during growth on non-selective plates will be insensitive to the negative selections by 5-FOA and α-aminoadipate. After mutagenesis, however, cells that have aquired a mutation which makes *ABP1* essential will be unable to lose the plasmid, and will therefore fail to form colonies on either α-aminoadipate or 5-FOA plates.

Table II. Complementation Analysis of ABP1-requiring mutants

Group	Gene	Number of alleles (Ts^-)
I	*SLA1*	13 (5)
II	*SLA2*	5 (5)
III	*SAC6*	4 (4)

For each complementation group, the gene name, total number of alleles, and number of temperature-sensitive alleles ( ) are shown.

We tested ~25,000 ethylmethanesulfonate-mutagenized colonies for their ability to grow on α-aminoadipate plates. Colonies (1148) which showed reduced growth were picked. These strains were then analyzed for their ability to grow on plates which contained 5-FOA. A total of 148 colonies failed to grow under both negative selection schemes and were thus good candidates for *ABP1*-requiring mutants. After three rounds of backcrossing, 24 independent strains showed segregation of a single nuclear mutation that made the cells dependent on pDD13 for their growth. The other 124 strains appeared to require multiple mutations to create the plasmid dependence, or had severe defects in their ability to sporulate, and were not studied further. The 24 well-behaved strains were also tested for their ability to grow at both high (37°C) and low (14°C) temperatures, and 14 strains showed a Ts^- growth defect genetically linked to the α-aminoadipate/5-FOA sensitivity (Table II). No cold-sensitive mutations (Cs^-) were found. Two of these 24 strains could not be complemented by a plasmid which carried only the *LYS2* and *ABP1* genes, and were subsequently shown to require the *URA3* gene for their growth (N. Machin, unpublished observations).

To determine the number of loci that were represented by the 22 *ABP1*-requiring mutant strains, a complementation test was performed. Diploids created by crossing the haploid single mutants (see Materials and Methods) were tested for their ability to grow on 5-FOA. All of the mutations isolated were found to be recessive. The 22 strains fell into three complementation groups (Table II). The four mutations in complementation group III are new alleles of *SAC6*, a gene which encodes an actin filament–bundling protein that is the yeast homolog of fimbrin (Adams et al., 1989, 1991). This was determined by a failure of these strains to complement a null allele of *SAC6*, and additionally by demonstrating linkage to a marked *SAC6* locus (data not shown). The two other complementation groups, termed *SLA1* and *SLA2*, contained 13 and five alleles, respectively.

Isolation and Sequence Analysis of the SLA1 and SLA2 Genes

The *SLA1* and *SLA2* genes were isolated by complementing the temperature sensitivity of mutant alleles of these genes (see Materials and Methods). For *SLA1*, targeted integration was used to show that the cloned DNA represents the mutant locus; for *SLA2*, an *sla2* gene disruption mutant (see below) was mated to an *sla2* mutant isolated in the original screen and spore analysis was used to prove linkage (see Materials and Methods). In each case, deletion analysis and subcloning were used to identify the minimum complementing frag-

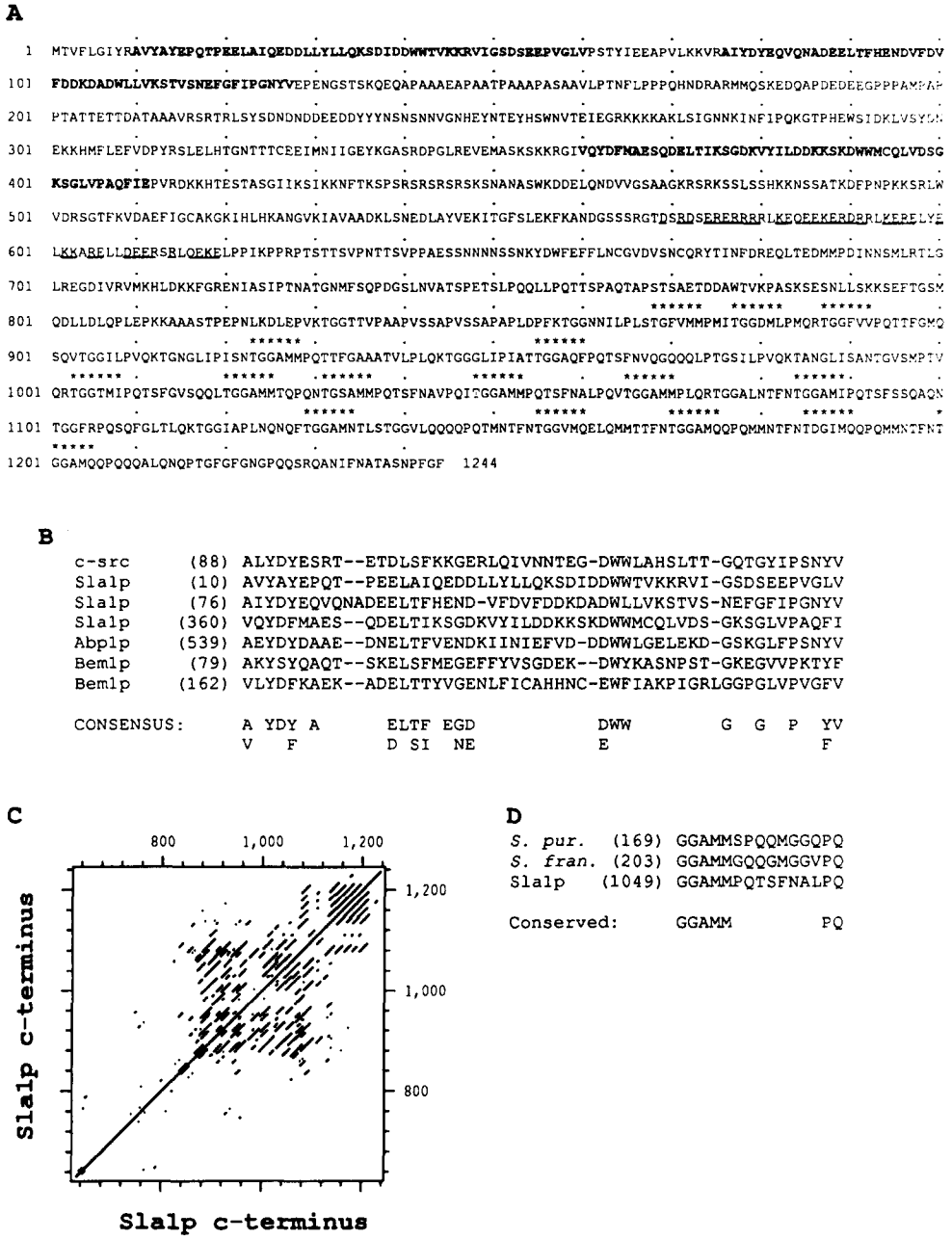

Figure 1. Predicted amino acid sequence of Slalp. (*A*) The predicted sequence of Slalp is shown in single letter amino acid code with the three SH3 domains in bold type. The region of highest charge density is underlined, and asterisks overlie the COOH-terminal core repeats. (*B*) Comparison of the SH3 domains from c-src and three yeast proteins. Top line of the consensus sequence is found in at least four of the seven SH3 domains shown, and the lower line is either a conservative substitution (e.g., E/D) of the primary residue, or found in at least two of the variant sequences shown here. Numbers in brackets refer to the position of the first amino acid of the SH3 domain within the identified protein. (*C*) Dot-plot display of repeated nature of Slalp. The COOH terminus of Slalp (residues 622–1244) is shown compared to itself using the GCG computer software Compare program with a window of 20 and stringency of 13. (*D*) Comparison of one extended repeat from Slalp to the related region of bindins from *Strongelocentrotus purpuratus* (*S. pur.*) (Gao et al., 1986) and *Strongelocentrotus franciscanis* (*S. fran.*) (Minor et al., 1991). The *SLA1* sequence data are available from EMBL under accession number Z22810.

ment, and the nucleotide sequence of the fragment was then determined. The sequences of the predicted protein products are shown in Figs. 1 and 2.

The *SLA1* gene contains a 1244 amino acid open reading frame that could encode a protein of 136 kD. Slalp shares structural homology with Abplp; Abplp has one SH3 domain, while Slalp has three of these domains (Fig. 1, *A* and *B*). Another interesting feature of Slalp is a repeat structure found in the COOH terminus, including numerous elements with the core TGGAMMP (Fig. 1, *A* and *C*). This region is nearly devoid of charged residues, with only three acidic and eight basic residues in the COOH-terminal 386 amino acids. Database searches with this sequence identified significant similarity to a region of the sea urchin sperm adhesion protein bindin (Fig. 1 *D*), although many of the Slalp repeats are more divergent and/or are truncated (Fig. 1 *A*). In striking contrast to the COOH terminus, the central third of Slalp is highly charged; one stretch of 50 amino acids contains 37 (74%) charged residues (Fig. 1 *A*).

The *SLA2* gene sequence predicts a 109-kD protein product of 968 amino acids (Fig. 2). A database search identified significant similarity between Sla2p and a *Caenorhabditis elegans* talinlike protein (Genpept accession No. celzk370–3; Bob Waterston, personal communication). The sequences are 22% identical and 34% similar in a pairwise alignment. The COOH termini of these proteins are more highly related, with 34% identity and 46% similarity over the last 200 residues. In addition, the COOH termini of both these sequences are related to murine talin (Rees et al., 1990). Sla2p is 28% identical and 36% similar to murine talin over this same 200 amino acids (Fig. 2). Several regions (e.g., GL[I/L]SAA and [V/I]AAST[I/A]QL, beginning at residues 818 and 861 of Sla2p, respectively) are well conserved in all three proteins.

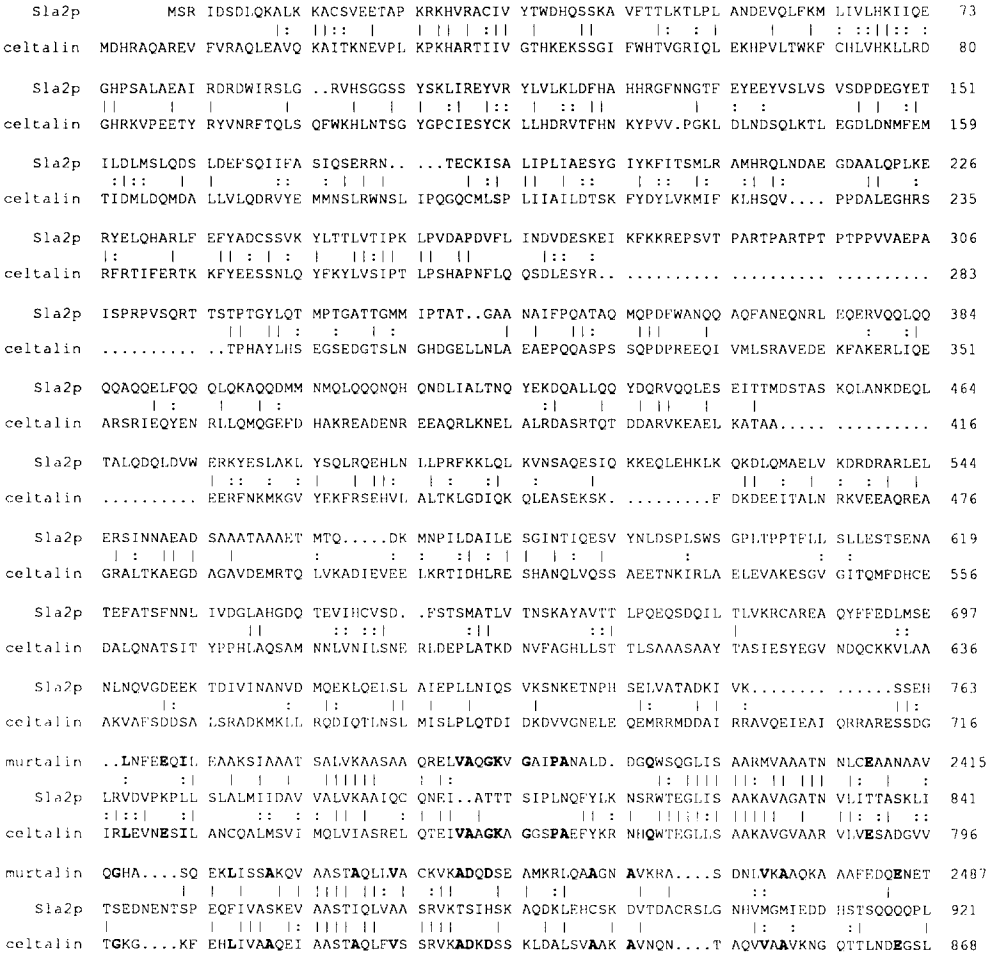

Figure 2. Predicted amino acid sequence of Sla2p and comparison with *Caenorhabditis elegans* talinlike sequence (*celtalin*) and murine talin (*murtalin*). Due to the length of murine talin and the absence of significant similarity to either Sla2p or celtalin in the NH_2-terminal 80% of the protein, only its COOH terminus is compared. Identities are indicated by a bar (|), and conserved amino acids (*D,E*; *M, I, V, L, C*; *K, R*; *Y, F*) are shown by a colon (:). At positions where only murine talin and the *C. elegans* talinlike sequence are identical, these residues are shown in bold. The *SLA2* sequence data are available from EMBL under accession number Z22811.

Null Mutations in SLA1 and SLA2 Cause Morphological Defects

To determine the in vivo roles of Slalp and Sla2p, homologous recombination was used to delete one copy of *SLA1* and *SLA2* (independently) in wild-type diploid strains (see Materials and Methods), and the heterozygous diploids were then sporulated. Deletions of either *SLA1* or *SLA2* make cells temperature sensitive for growth, with the *sla2* deletion strains showing a narrower permissive temperature range (Fig. 3). *sla1* deletion mutant strains grow well at 34°C, while *sla2*Δ mutants fail to grow at 34°C and grow poorly at 30°C.

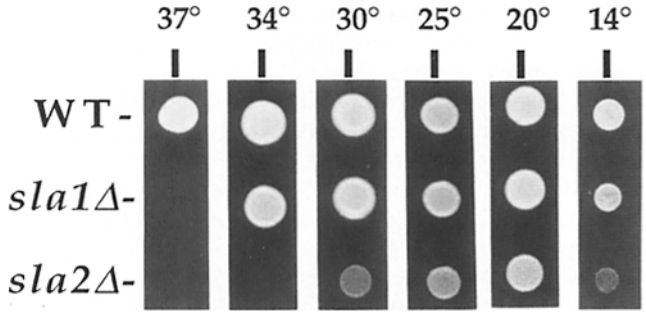

Figure 3. sla1 and *sla2* deletion strains show temperature-sensitive growth defects. Haploid wild type (*WT*), *sla1*Δ, and *sla2*Δ (DDY 494, 495, 496) strains were replica plated and grown for 36 h (37°C, 34°C), 48 h (30°C, 25°C), 72 h (20°C), or 5 d (14°C) on YPD plates before being photographed as shown.

sla1 and *sla2* null strains also show morphological defects, despite the fact that these cells have an intact copy of *ABP1*. Wild-type diploid strains are ellipsoid in shape (Fig. 4, *a* and *c*). In contrast, *sla2* null strains are spherical in appearance, even at 20°C (Fig. 4 *i*). In addition, DAPI staining showed that a small number of cells (~3%) are multinucleate (data not shown). At the non-permissive temperature of 37°C, *sla2* null strains grow isotropically and become significantly larger than wild-type cells (Fig. 4 *k*). After 90 min at the non-permissive temperature, ~20% of the cells are multinucleate (Fig. 4 *l*). The defect in *sla1* strains is less severe than *sla2* strains at 20°C, although the cells are noticeably more spherical than wild type (Fig. 4 *e*). At non-permissive temperatures (37°C) *sla1* null strains show more pronounced morphological defects (Fig. 4 *g*). A variety of abnormalities are seen, including round cells, cells which have abnormal surface protrusions, and an increase in the range of cell sizes. In addition, ~20% of the cells appear heavily vacuolated un-

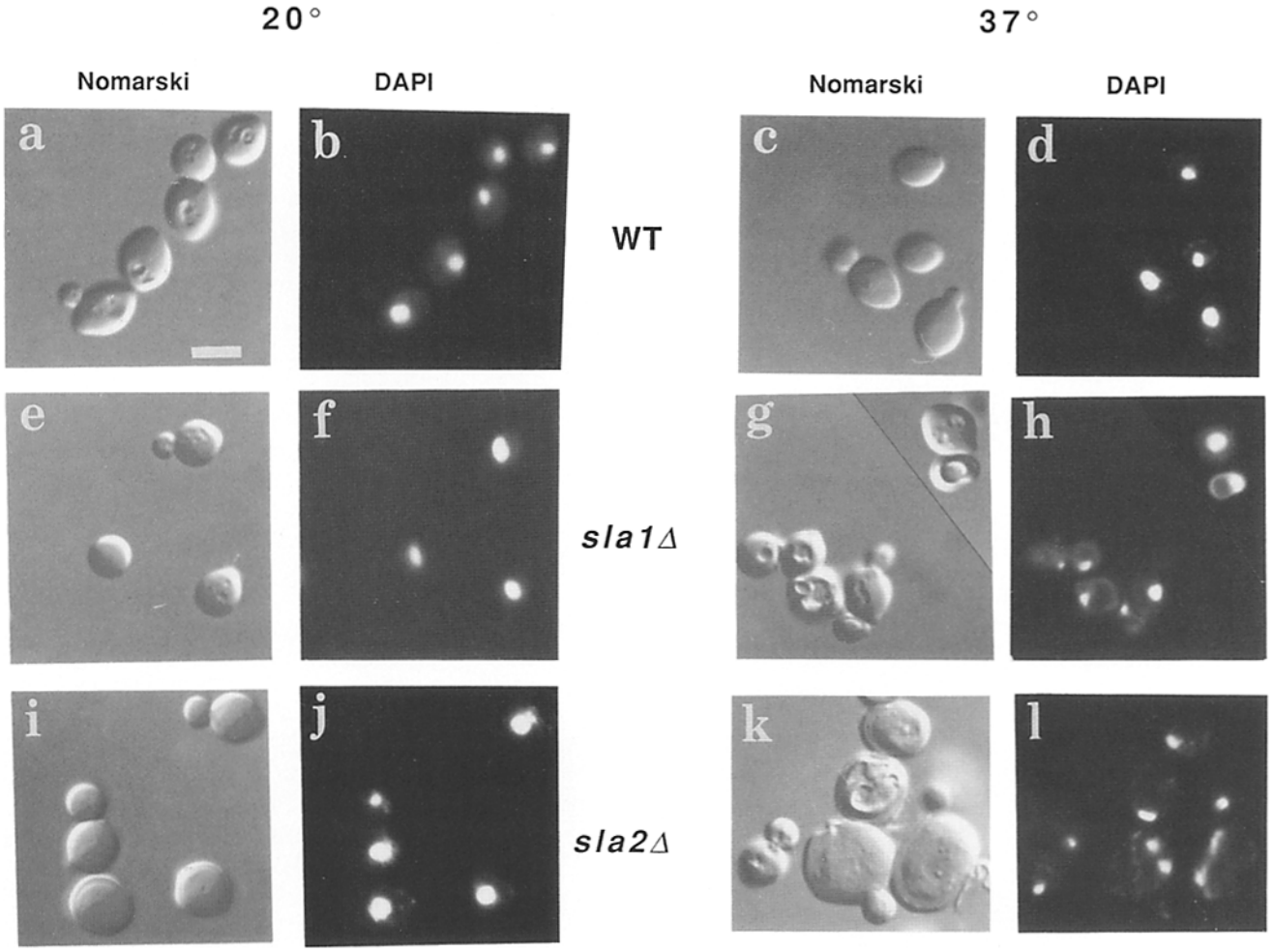

Figure 4. slal and *sla2* deletion strains show defects in morphogenesis. Wild-type (DDY 288) (*a–d*), *slal*Δ (DDY 485) (*e–h*), and *sla2*Δ (DDY 540) (*i–l*) diploid cells were grown at 20°C overnight and then shifted to 37°C for 90 min. Cells were fixed and mounted on slides with their cell walls intact. Nuclei are visualized using DAPI. Scale bar in *a* is 5 μm and applies to all panels.

der Nomarski optics, and lose nuclear integrity as evaluated by DAPI staining (Fig. 4, *g* and *h*). The morphologic defects of *slal*Δ and *sla2*Δ mutants, like those seen with other mutants defective in cytoskeletal proteins (Liu and Brescher, 1989; Amatruda et al., 1990; Adams et al., 1991), are heterogeneous. Further studies using synchronized populations of cells will be required to determine if these genes function at a particular phase in the cell cycle or are required continuously throughout the budding process.

slal and sla2 Mutants Have Unique Cytoskeletal Defects

SLA1 and *SLA2* are both required for the normal organization of the cortical cytoskeleton. The actin cytoskeleton of wild-type cells shows two identifiable structures. Actin cables are arrayed parallel to the mother-bud axis, while cortical patches are highly polarized, being concentrated at the bud surface during vegetative growth (Fig. 5, *a* and *c*) (Adams and Pringle, 1984; Kilmartin and Adams, 1984). In *slal* null strains, a dramatic defect exists in the formation of the cortical cytoskeleton, even at the nominally permissive temperature of 20°C. Instead of the regular punctate staining seen in wild-type cells, fewer, larger "chunks" of actin are visible in all cells (Fig. 5 *e*). Despite this defect, the cortical actin structures are properly polarized to the bud surface. These structures are likely to be composed of actin filaments as they stain with rhodamine–phalloidin, a polymer-specific probe (data not shown). Actin cables are properly oriented in *slal* null strains, although their fluorescence intensity appears reduced compared to staining in wild-type cells. Upon shift to non-permissive temperature (37°C), the cortical actin structures become delocalized, and cell death becomes apparent based on phase microscopy observations (not shown). In addition, ~5–10% of the cells show other defects in actin organization, such as bars of actin and actin staining in the nucleus (data not shown).

The *sla2*Δ strain shows a different defect in its cortical cytoskeleton. This strain shows a delocalization of cortical structures, even at 20°C (Fig. 5 *i*). Cells also show an apparent increase in the number of cortical structures per unit surface area. Cables are present in these cells, though they appear to be oriented randomly and are often obscured by the large number of cortical structures. Upon shift to the non-permissive temperature of 37°C, *sla2*Δ cells increase in size, and after 90 min, as stated above, ~20% of the cells are multinucleate (Fig. 5, *k* and *l*).

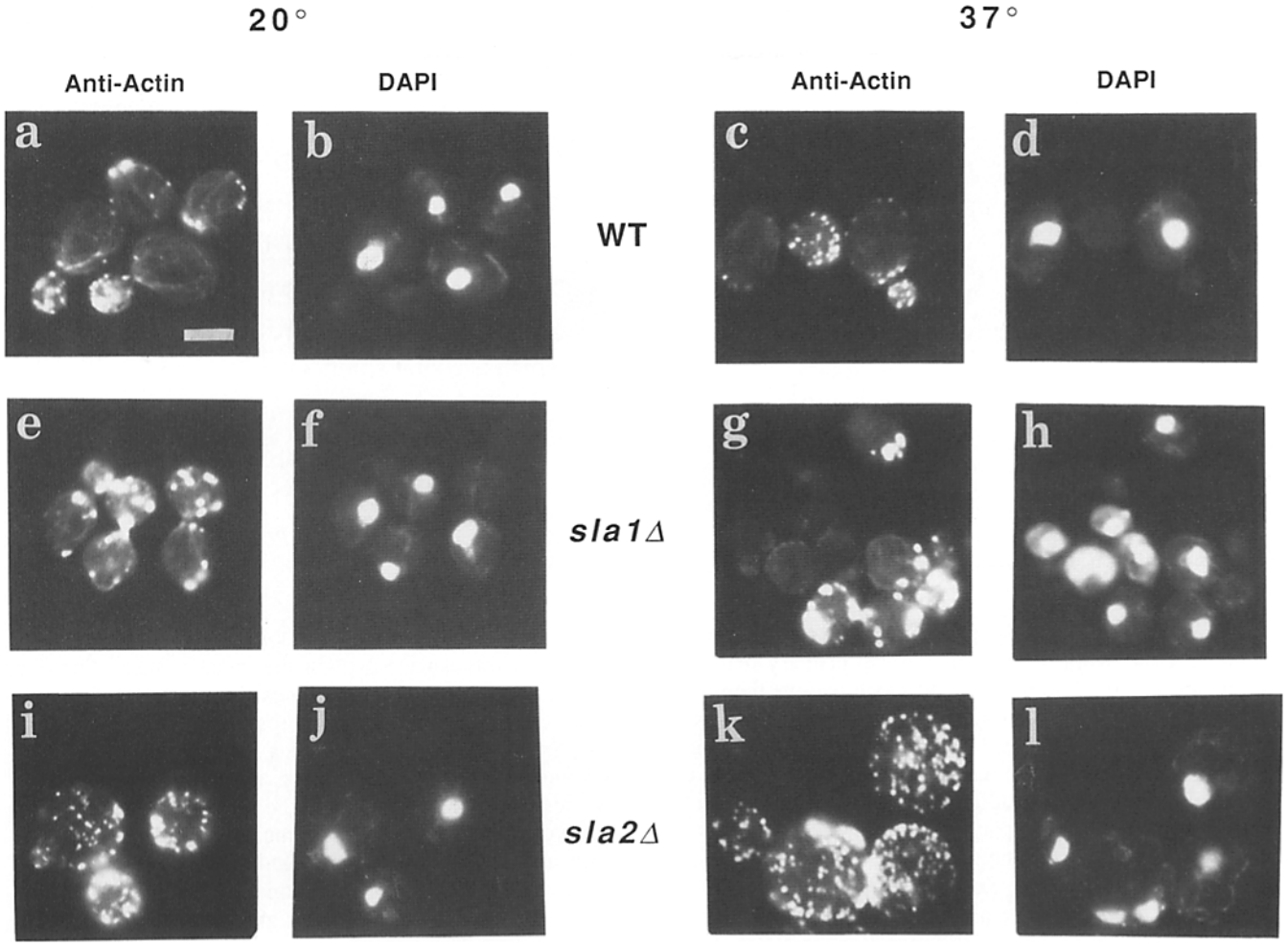

Figure 5. slal and *sla2* deletion strains show defects in the formation and organization of the cortical actin cytoskeleton. Wild-type (DDY288) (*a–d*), *slal*Δ (DDY 485) (*e–h*) and *sla2*Δ (DDY 540) (*i–l*) cells were grown at 20°C and then shifted to 37°C for 90 min. Cells were stained with anti-actin antibodies or DAPI, as indicated. Cells in *g* that have lost actin staining appear dead based on phase microscopy observations (data not shown). Scale bar in *a* is 5 μm and applies to all panels.

Genetic Interactions between SLA1, SLA2, and SAC6

Null mutations in the nonessential *SLA1*, *SLA2*, and *SAC6* genes all create a requirement for the *ABP1* gene, although some viable double-mutant spores that are severely compromised for their ability to grow do germinate (Adams et al., 1993, and data not shown). To determine whether the *SLA1*, *SLA2*, and *SAC6* genes showed any other examples of functional interactions, heterozygous diploids for all three pair-wise combinations of null alleles were sporulated, and the dissected tetrads were analyzed for their ability to grow at a variety of temperatures. *sla2*Δ-*sac6*Δ double-mutant spores are extremely sick, with >30% inferred spore inviability (Fig. 6 *B*). The *sla2*Δ-sac6Δ double-mutant spores that do germinate do not show growth after 72 h at 20°C when replica plated (data not shown). *slal*Δ-sac6Δ double mutants are viable, Ts^- strains that show the same permissive temperature range as the single mutants (Fig. 6 *C*, and data not shown). The *slal*Δ -*sla2*Δ double-mutant strains are viable, but are sicker than null alleles of either *SLA1* or *SLA2* (Fig. 6 *A*). Double-mutant strains grow poorly at 20°C and 25°C, and fail to grow at 30°C, a temperature at which both *slal* and *sla2* single mutant strains are viable (Fig. 3, and data not shown). The interactions between mutations in *ABP1*, *SAC6*, *SLA1*, and *SLA2* are summarized in Fig. 7.

Discussion

In this study we have identified proteins required for cortical cytoskeletal function based on their interactions in the living cell. Mutations in three genes can create a requirement for the cortical actin-binding protein Abplp in *S. cerevisiae.* One of these genes, *SAC6*, encodes an actin filament-bundling protein previously shown to be a component of the cortical cytoskeleton. The two new genes isolated in this screen, *SLA1* and *SLA2*, have homologies which suggest that they are novel components or regulators of the actin cytoskeleton. Phenotypic analysis of *slal*Δ and *sla2*Δ mutants confirms that these genes, unlike *ABP1*, are essential for proper membrane cytoskeleton assembly and morphogenesis.

One unexpected finding is the structural diversity of proteins that, based on genetic interactions, define a functionally overlapping set. For example, although null mutations

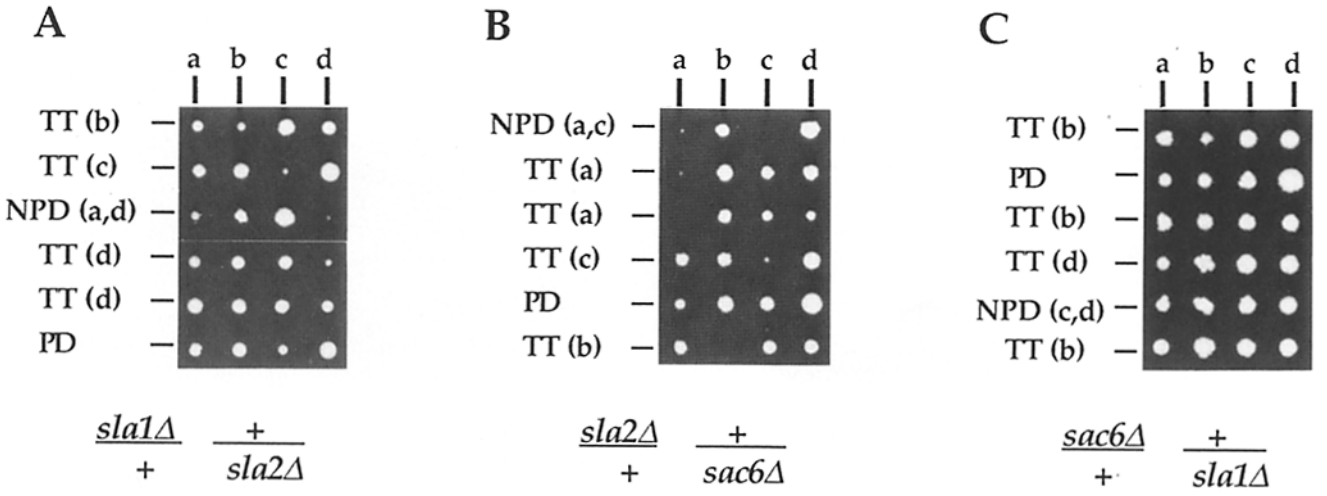

Figure 6. Genetic interactions between *sla1*, *sla2*, and *sac6* deletion mutations. (*A–C*) Heterozygous diploids containing all three pair-wise combinations of null mutant alleles were sporulated, dissected and grown for 4 d at 25°C before being photographed. Colonies were then replica plated to determine the segregation of the marked mutant alleles. Tetrad genotype (*TT*, tetratype; *PD*, parental ditype; and *NPD*, non-parental ditype) is indicated, and the identity of the double mutant spore(s) is shown in parenthesis.

in *SAC6* and *ABP1* are synthetically lethal, their protein products show no similarity at the level of primary structure. Importantly, not all double-mutant combinations within the group of four genes studied here show a negative synergism at 25°C (e.g., *sac6Δ-sla1Δ*). This demonstrates that the contributions of Sac6p, Sla1p, and Sla2p to cell viability are not identical, and therefore that the nature of their redundancies with Abp1p may also be distinct.

Understanding the synthetic–lethal relationships between mutations in *ABP1*, *SAC6*, *SLA1*, and *SLA2* could shed light on the roles that their protein products play in the regulation of the cortical cytoskeleton. Null mutations in *SAC6*, *SLA1*, and *SLA2* all result in inviability at 37°C, indicating that the yeast actin cytoskeleton is functionally compromised at high temperatures without its full complement of these accessory proteins. How can we explain the genetic interactions between mutations in this set of genes? One model is suggested by biochemical analyses of cytoskeletal components. In vitro, many actin-binding proteins are multifunctional (Pollard and Cooper, 1986; Hartwig and Kwiatkowski, 1991), and perhaps this is reflected in the genetic relationships we observe. Thus, Abp1p might be multifunctional, and Sac6p, Sla1p, and Sla2p might be redundant with different biochemical activities of Abp1p. An additional point that must be considered is that *abp1* null mutants grow well at 37°C. It may be that the temperature sensitivity of strains lacking either Sac6p, Sla1p, or Sla2p is due to the loss of functions that are not redundant with Abp1p. In support of this possibility, we have isolated eight alleles of *SLA1* which create a dependence on *ABP1* but do not cause cells to become Ts^-. These alleles may be specifically deficient in an Sla1p activity which is redundant with Abp1p while retaining other functions necessary for growth at high temperature.

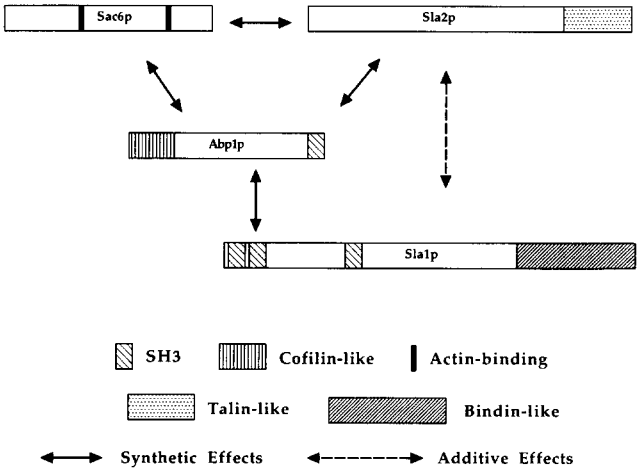

Figure 7. Schematic diagram of the protein structures of Abp1p, Sla1p, Sla2p, and Sac6p, and the genetic interactions observed between mutations in their corresponding genes. "Synthetic Effects" (e.g., *sla2Δ*-sac6Δ) are distinguished from "Additive Effects" (e.g., *sla1Δ*-sla2Δ) to signify that the former class of interactions has significantly more severe effects on cell growth and/or viability than the latter (see text).

On a biochemical level, it is possible that the synthetic–lethal interactions are due to the loss of activities that exert similar effects on the actin cytoskeleton, albeit through different mechanisms. For example, it is possible that proteins which cap the ends of filaments and proteins which bind to the sides of filaments might each slow actin filament depolymerization in vivo. In addition, the function of the yeast actin cytoskeleton can be affected by gene dosage (Drubin et al., 1988; Wertman et al., 1992), and this may help to explain the results of our screen. In this case, Sac6p, Abp1p, and Sla2p might all have similar effects on actin organization, and cell viability would depend on the expression of at least two of these proteins. Sac6p is known to bundle actin filaments (Adams et al., 1991). In vitro assays to determine the effects that Abp1p, Sla1p, and Sla2p have on actin assembly may provide clues to help understand the genetically defined redundancies. While all of these gene products can affect the actin cytoskeleton (Drubin et al., 1988; Adams et al., 1991; Fig. 5), it is also possible that the lethality of certain double-mutant combinations is the result of deficiencies that are unrelated to the effects these proteins have on the or-

ganization of actin. For example, some mutant combinations might hinder the integration of cortical events with those occurring in other compartments of the cell.

What role do *SLA1* and *SLA2* play in polarized growth and the regulation of the actin cytoskeleton? Mutations in both genes affect the ellipsoid cell shape characteristic of wild-type diploid cells, with the mutants growing more spherically. Immunofluorescence experiments reveal striking defects in the cortical cytoskeletons of these strains. Significantly, the *sla1*Δ and *sla2*Δ defects are distinct, indicating that these genes play fundamentally different roles in the cell. The *sla1*Δ mutants show a unique defect in the formation of their cortical cytoskeleton. Previously, all mutations affecting the cortical actin cytoskeleton were found to cause a delocalization of wild-type actin structures (as judged by immunofluorescence experiments). In *sla1* null strains, a smaller number of F-actin structures are found at the cortex, and these structures appear larger in size. However, these aberrant structures are properly polarized to the growing bud. Sla1p might therefore be involved in controlling the size of the cortical patches, perhaps by regulating the nucleation of filaments at the cortex. A decrease in the number of actin nucleation sites might be expected to favor incorporation of monomeric actin onto preexisting filaments, resulting in fewer, larger structures. In contrast to *sla1*Δ strains, *sla2*Δ strains show a cytoskeletal phenotype more similar to mutations that affect cell polarity (e.g., *cdc42*, *cdc43*), where the cortical patches are uniformly distributed at the cell cortex rather than being concentrated in the bud, and cell growth is isotropic rather than polarized (Adams et al., 1990). Therefore, Sla2p might act in concert with proteins such as Cdc42p and Cdc43p to limit the region of cortical patch formation to the cortex of the bud.

A complete understanding of yeast morphogenesis will require determining how actin assembly is controlled both spatially and temporally. Sla1p contains three SH3 domains. Abp1p and Bem1p, other proteins implicated in polarized growth in *S. cerevisiae*, also contain SH3 domains (Drubin et al., 1990; Chenevert et al., 1992). This motif has been shown recently to bind specific ligands including 3BP-1, a protein which has a region of homology with rho GTPase activators of the bcr/N-chimaerin family (Cicchetti et al., 1992). Finding an SH3-ligand(s) in yeast might help establish a biochemical link between the bud site selection/polarity genes and the cytoskeleton (reviewed in Chant and Pringle, 1991; Drubin, 1991). Unlike *SLA1*, however, null mutations in *BEM1* are not lethal in combination with *abp1* null alleles (Chenevert, J., and D. A. Holtzman, unpublished observations), indicating that although these SH3-containing proteins all contribute to the development of cell polarity, distinctions exist between their specific functions. This is perhaps not surprising as various SH3 domains, while possessing several well-conserved consensus residues, do show significant divergence (Musacchio et al., 1992) and different affinities in their interactions with ligands (Cicchetti et al., 1992; Ren et al., 1993).

Another striking feature of Sla1p is the extensive repeat structure of the COOH terminus that shows limited homology to bindins, a family of species-specific sperm adhesion proteins from sea urchins. Bindins have been shown to interact directly with phospholipid vesicles and to facilitate vesicle fusion in vitro (Glabe, 1985*a*, *b*). It is interesting to note that the amino acid composition of this sequence is hydrophobic, a characteristic of viral fusion proteins (White, 1992), although no activity has yet been ascribed to this region of bindin. Perhaps the COOH terminus of Sla1p associates with the plasma membrane, or contributes to localized vesicle fusion at the growing surfaces of the cell.

Small GTP binding proteins of the rho family (*CDC42*, *RHO3*, *RHO4*) are required for bud site formation and the asymmetric disposition of the cortical actin cytoskeleton (Adams et al., 1990; Johnson and Pringle, 1990; Matsui and Toh-e, 1992). In fibroblasts, rho proteins are essential for mitogen-induced formation of focal adhesions (Ridley and Hall, 1992), protein complexes that link actin stress fibers to the plasma membrane and extracellular matrix (reviewed in Burridge et al., 1988). It is intriguing that the other gene isolated in our screen shows significant similarity to the COOH terminus of talin, a protein recruited to focal adhesions by the actions of rho proteins and capable of nucleating actin filament assembly in vitro (Ridley and Hall, 1992; Muguruma et al., 1990; Kaufmann et al., 1991). By analogy, rho-like proteins in *S. cerevisiae* might regulate the formation of a cortical protein complex of which Sla2p is a component, and this in turn could influence the local assembly of the actin cytoskeleton. The in vivo activity of rho proteins is likely to be downregulated by bcr-GAP molecules (Diekmann et al., 1991; Settleman et al., 1992), and this interaction might be modulated by SH3-containing proteins. It is now important to determine the in vivo localizations of both Sla proteins, and to determine if the *sla1* and *sla2* mutations affect the localization of other components of the cortical cytoskeleton.

In conclusion, the actin cytoskeleton of *S. cerevisiae* provides a facile genetic route to examine the complexities of the eukaryotic cell cortex. Our identification of proteins required for membrane cytoskeletal function and assembly in vivo provides a step toward developing a deeper understanding of the biochemical basis for the genetic redundancies in the cytoskeleton, and the way intracellular and extracellular signals are integrated to regulate cytoskeletal assembly and cell polarity.

We are grateful to Tom Lila, John Pringle, and Randy Schekman for their helpful comments on this manuscript. We are particularly indebted to Don Rio for generous access to his oligonucleotide synthesis facility, Eileen Beall for help with synthesis of primers, Mellissa Cobb for assistance with computer sequence analysis, and Nate Machin for help with this project. We would also like to thank Alison Adams for strains and advice on genetics, Colin Watanabe for help in finding the homology of Sla1p with bindin, and Georjana Barnes, Susan Marquesee, Judith White, Charles Glabe, and Jasper Rees for discussions on various aspects of this project.

D. A. Holtzman and S. Yang were supported by training grants from the National Institutes of Health. This work was supported by grants to D. G. Drubin from the National Institute of General Medical Sciences (GM-42759) and the Searle Scholars Program/The Chicago Community Trust.

Received for publication 22 March 1993 and in revised form 18 May 1993.

References

Adams, A. E. M., and J. R. Pringle. 1984. Relationship of actin and tubulin distribution to bud growth in wild-type and morphogenetic-mutant *Saccharomyces cerevisiae*. *J. Cell Biol.* 98:934–945.

Adams, A. E. M., D. Botstein, and D. G. Drubin. 1989. A yeast actin-binding protein is encoded by *SAC6*, a gene found by suppression of an actin mutation. *Science (Wash. DC)*. 243:231–233.

Adams, A. E. M., D. I. Johnson, R. M. Longnecker, B. F. Sloat, and J. R.

Pringle. 1990. *CDC42* and *CDC43*, two additional genes involved in budding and the establishment of cell polarity in the yeast *Saccharomyces cerevisiae*. *J. Cell Biol.* 111:131–142.

Adams, A. E. M., D. Botstein, and D. G. Drubin. 1991. Requirement of yeast fimbrin for actin organization and morphogenesis in vivo. *Nature (Lond.).* 354:404–408.

Adams, A. E. M., J. A. Cooper, and D. G. Drubin. 1993. Unexpected combinations of null mutations in genes encoding the actin cytoskeleton are lethal in yeast. *Mol. Biol. Cell.* 4:459–468.

Amatruda, J. F., J. F. Cannon, K. Tatchell, C. Hug, and J. A. Cooper. 1990. Disruption of the actin cytoskeleton in yeast capping protein mutants. *Nature (Lond.).* 344:352–354.

Ausubel, F. M., R. Brent, R. E. Kingston, D. D. Moore, J. G. Seidman, J. A. Smith, and K. Struhl. 1989. Short Protocols in Molecular Biology. Greene Publishing Associates and Wiley-Interscience, New York. 387 pp.

Basson, M. E., R. L. Moore, J. O'Rear, and J. Rine. 1987. Identifying mutations in duplicated functions in *Saccharomyces cerevisiae*: recessive mutations in HMG-CoA reductase genes. *Genetics.* 117:645–655.

Bender, A., and J. R. Pringle. 1991. Use of a screen for synthetic-lethal and multicopy-suppressee mutants to identify two new genes involved in morphogenesis in *Saccharomyces cerevisiae*. *Mol. Cell. Biol.* 11:1295–1305.

Boeke, J. D., F. Lacroute, and G. R. Fink. 1984. A positive selection for mutants lacking orotidine-5′-phosphate decarboxylase activity in yeast: 5-fluoro-orotic acid resistance. *Mol. Gen. Genet.* 197:345–346.

Burridge, K., K. Fath, T. Kelly, G. Nuckolls, and C. Turner. 1988. Focal adhesions: transmembrane junctions between the extracellular matrix and the cytoskeleton. *Ann. Rev. Cell Biol.* 4:487–525.

Chant, J., and J. R. Pringle. 1991. Budding and cell polarity in *Saccharomyces cerevisiae*. *Curr. Opin. Genet. Dev.* 1:342–350.

Chattoo, B. B., and F. Sherman. 1979. Selection of *lys2* mutants of the yeast *Saccharomyces cerevisiae* by the utilization of alpha-aminoadipate. *Genetics.* 93:51–65.

Chenevert, J., K. Corrado, A. Bender, J. R. Pringle, and I. Herskowitz. 1992. A yeast gene (*BEM1*) necessary for cell polarization whose product contains two SH3 domains. *Nature (Lond.).* 356:77–79.

Cicchetti, P., B. J. Mayer, G. Thiel, and D. Baltimore. 1992. Identification of a protein that binds to the SH3 region of *abl* and is similar to *bcr* and GAP-rho. *Science (Wash. DC).* 257:803–806.

De Lozanne, A., and J. A. Spudich. 1987. Disruption of the *Dictyostelium* myosin heavy chain gene by homologous recombination. *Science (Wash. DC).* 236:1086–1091.

Diekmann, D., S. Brill, M. D. Garrett, N. Totty, J. Hsuan, C. Monfries, C. Hall, L. Lim, and A. Hall. 1991. *Bcr* encodes a GTPase-activating protein for p21rac. *Nature (Lond.).* 351:400–402.

Drubin, D. G. 1991. Development of cell polarity in budding yeast. *Cell.* 65:1093–1096.

Drubin, D. G., K. G. Miller, and D. Botstein. 1988. Yeast actin-binding proteins: Evidence for a role in morphogenesis. *J. Cell Biol.* 107:2551–2561.

Drubin, D. G., J. Mulholland, Z. Zhimin, and D. Botstein. 1990. Homology of a yeast actin-binding protein to signal transduction proteins and myosin-I. *Nature (Lond.).* 343:288–290.

Field, C., and R. Schekman. 1980. Localized secretion of acid phosphatase reflects the pattern of cell surface growth in *Saccharomyces cerevisiae*. *J. Cell Biol.* 86:123–128.

Gallwitz, D., and I. Sures. 1980. Structure of a split yeast gene: complete nucleotide sequence of the actin gene in *Saccharomyces cerevisiae*. *Proc. Natl. Acad. Sci. USA.* 77:2546–2550.

Gao, B., L. E. Klein, R. J. Britten, and E. H. Davidson. 1986. Sequence of mRNA coding for bindin, a species-specific sea urchin sperm protein required for fertilization. *Proc. Natl. Acad. Sci. USA.* 83:8634–8638.

Glabe, C. G. 1985*a*. Interaction of the sperm adhesive protein, bindin, with phospholipid vesicles. I. Specific association of bindin with gel-phase phospholipid vesicles. *J. Cell Biol.* 100:794–799.

Glabe, C. G. 1985*b*. Interaction of the sperm adhesive protein, bindin, with phospholipid vesicles. II. Bindin induces the fusion of mixed-phase vesicles that contain phosphatidylcholine and phosphatidylserine in vitro. *J. Cell Biol.* 100:800–806.

Hartwig, J. H., and D. J. Kwiatkowski. 1991. Actin-binding proteins. *Curr. Opin. Cell Biol.* 3:87–97.

Ito, H., Y. Fukuda, K. Murata, and A. Kimura. 1983. Transformation of intact yeast cells treated with alkali cations. *J. Bacteriol.* 153:163–168.

Johnson, D. I., and J. R. Pringle. 1990. Molecular characterization of *CDC42*, a *Saccharomyces cerevisiae* gene involved in the development of cell polarity. *J. Cell Biol.* 111:143–152.

Kaufmann, S., T. Piekenbrock, W. H. Goldmann, M. Bärmann, and G. Isenberg. 1991. Talin binds to actin and promotes filament nucleation. *FEBS (Fed. Eur. Biochem. Soc.) Lett.* 284:187–191.

Kilmartin, J., and A. E. M. Adams. 1984. Structural rearrangements of tubulin and actin during the cell cycle of the yeast *Saccharomyces*. *J. Cell Biol.* 98:922–933.

Koch, C. A., D. Anderson, M. F. Moran, C. Ellis, and T. Pawson. 1991. SH2 and SH3 domains: elements that control interactions of cytoplasmic signaling proteins. *Science (Wash. DC).* 252:668–674.

Liu, H., and A. Bretscher. 1989. Disruption of the single tropomyosin gene in yeast results in the disappearance of actin cables from the cytoskeleton. *Cell.* 57:233–242.

Luna, E. J., and A. L. Hitt. 1992. Cytoskeleton-plasma membrane interactions. *Science (Wash. DC).* 258:955–964.

Matsui, Y., and A. Toh-e. 1992. Yeast *RHO3* and *RHO4* ras superfamily genes are necessary for bud growth, and their defect is suppressed by a high dose of bud formation genes *CDC42* and *BEM1*. *Mol. Cell. Biol.* 12:5690–5699.

Minor, J. E., D. R. Fromson, R. J. Britten, and E. H. Davidson. 1991. Comparison of the bindin proteins of *Strongylocentrotus franciscanus*, *Strongylocentrotus purpuratus*, and *Lytechinus variagatus*: sequences involved in the species specificity of fertilization. *Mol. Biol. Evol.* 8:781–795.

Moon, A. L., P. A. Janmey, K. A. Louie, and D. G. Drubin. 1993. Cofilin is an essential component of the yeast cortical cytoskeleton. *J. Cell Biol.* 120:421–435.

Muguruma, M., S. Matsumura, and T. Fukazawa. 1990. Direct interactions between talin and actin. *Biochem. Biophys. Res. Commun.* 171:1217–1223.

Musacchio, A., M. Noble, R. Pauptit, R. Wierenga, and M. Saraste. 1992. Crystal structure of a Src-homology 3 (SH3) domain. *Nature (Lond.).* 359:851–855.

Ng, R., and J. Abelson. 1980. Isolation of the gene for actin in *Saccharomyces cerevisiae*. *Proc. Natl. Acad. Sci. USA.* 77:3912–3916.

Novick, P., and D. Botstein. 1985. Phenotypic analysis of temperature-sensitive yeast actin mutants. *Cell.* 40:405–416.

Pollard, T. D., and J. A. Cooper. 1986. Actin and actin-binding proteins. A critical evaluation of mechanisms and functions. *Ann. Rev. Biochem.* 55:987–1035.

Pringle, J. R., A. E. M. Adams, D. G. Drubin, and B. K. Haarer. 1991. Immunofluorescence methods for yeast. *Methods Enzymol.* 194:565–602.

Read, E. B., H. H. Okamura, and D. G. Drubin. 1992. Actin- and tubulin-dependent functions during *Saccharomyces cerevisiae* mating projection formation. *Mol. Biol. Cell.* 3:429–444.

Rees, D. J. G., S. E. Ades, S. J. Singer, and R. O. Hynes. 1990. Sequence and domain structure of talin. *Nature (Lond.).* 347:685–689.

Ren, R., B. J. Mayer, P. Cicchetti, and D. Baltimore. 1993. Identification of a ten-amino acid proline-rich SH3 binding site. *Science (Wash. DC).* 259:1157–1161.

Ridley, A. J., and A. Hall. 1992. The small GTP-binding protein rho regulates the assembly of focal adhesions and actin stress fibers in response to growth factors. *Cell.* 70:389–399.

Rose, M. D., P. Novick, J. H. Thomas, D. Botstein, and G. R. Fink. 1987. A *Saccharomyces cerevisiae* genomic plasmid bank based on a centromere-containing shuttle vector. *Gene.* 60:237–243.

Rothstein, R. J. 1983. One-step gene disruption in yeast. *Methods Enzymol.* 101:202–211.

Sanger, F., S. Nicklen, and A. R. Coulson. 1977. DNA sequencing with chain-terminating inhibitors. *Proc. Natl. Acad. Sci. USA.* 74:5463–5467.

Schiestl, R. H., and R. D. Gietz. 1989. High efficiency transformation of intact yeast cells using single stranded nucleic acids as a carrier. *Curr. Genet.* 16:339–346.

Schwartz, M. A. 1992. Transmembrane signalling by integrins. *Trends Cell Biol.* 2:304–308.

Settleman, J., C. F. Albright, L. C. Foster, and R. A. Weinberg. 1992. Association between GTPase activators for Rho and Ras families. *Nature (Lond.).* 359:153–154.

Sherman, F., G. R. Fink, and J. B. Hicks. 1986. Methods In Yeast Genetics. Cold Spring Harbor Laboratory, Cold Spring Harbor, New York. 186 pp.

Sikorski, R. S., and P. Hieter. 1989. A system of shuttle vectors and yeast host strains designed for efficient manipulation of DNA in *Saccharomyces cerevisiae*. *Genetics.* 122:19–27.

Wertman, K. F., D. G. Drubin, and D. Botstein. 1992. Systematic mutational analysis of the yeast *ACT1* gene. *Genetics.* 132:337–350.

White, J. M. 1992. Membrane fusion. *Science (Wash. DC).* 258:917–924.

Witke, W., M. Schleicher, and A. A. Noegel. 1992. Redundancy in the microfilament system: abnormal development of *Dictyostelium* cells lacking two F-actin cross-linking proteins. *Cell.* 68:53–62.

Yu, H., M. K. Rosen, T. B. Shin, C. Seidel-Dugan, J. S. Brugge, and S. L. Schreiber. 1992. Solution structure of the SH3 domain of src and identification of its ligand-binding site. *Science (Wash. DC).* 258:1665–1668.